

# Sparsity-promoting joint microseismic source collocation and source-time function estimation

Shashin Sharan<sup>1\*</sup>, Rongrong Wang<sup>1</sup>, Tristan van Leeuwen<sup>2</sup> and Felix J. Herrmann<sup>1</sup>

<sup>1</sup> Seismic Laboratory for Imaging and Modeling (SLIM), University of British Columbia

<sup>2</sup> Utrecht University

## SUMMARY

In this work, we propose a new method to simultaneously locate microseismic events (e.g., induced by hydraulic fracturing) and estimate the source signature of these events. We use the method of linearized Bregman. This algorithm focuses unknown sources at their true locations by promoting sparsity along space and at the same time keeping the energy along time in check. We are particularly interested in situations where the microseismic data is noisy, sources have different signatures and we only have access to the smooth background-velocity model. We perform numerical experiments to demonstrate the usability of the proposed method. We also compare our results with full-waveform inversion based microseismic event collocation methods. Our method gives flexibility to simultaneously get a more accurate source image along with an estimate of the source-time function, which carries important information on the rupturing process and source mechanism.

## INTRODUCTION

During hydraulic fracturing high-pressure fluid is injected through a well creating fractures in the rocks mainly containing shale (Montgomery and Smith, 2010). Shale contains oil traps but they are weakly connected due to the low permeability of shale. These fractures connect the oil traps, which ultimately enhances the oil productivity. In order to predict the production level of oil through these fracture induced reservoirs, it is extremely important to accurately map fracture propagation.

Hydraulic fracturing of rocks causes stress release, which eventually emits microseismic waves (Rutledge and Phillips, 2003). These waves carry important information about different source parameters such as source location, source origin time, source-time function etc. In microseismic imaging these induced seismic waves are recorded by surface receivers or receivers along a well. The resulting data is subsequently used to estimate different source parameters.

Traditional methods include travel time inversion, which relies on identification of different P and S components and traveltimes picking of first arrivals of P and S components (Thurber and Engdahl, 2000; Waldhauser and Ellsworth, 2000). Identification of different components and traveltimes picking of first arrivals is time consuming and can be extremely difficult in the presence of noise.

In recent years techniques have been developed that rely less or not at all on traveltimes picking (Rentsch et al., 2007). Also the focus has shifted to the methods based on imaging (McMechan, 2010; Gajewski and Tessmer, 2005; Sun et al., 2015) and full-waveform inversion (FWI) (Sjögreen and Petersson, 2014; Kaderli et al., 2015). These methods rely less on first-arrival picking and are more robust to noise.

Kaderli et al. (2015) use FWI to invert for both the source-time function and source location. This method is based on estimating both parameters in an alternating fashion. However, the source location estimated by this method looks diffused and the estimated source-time function is noisier compared to the true wavelet.

Sun et al. (2015) use a hybrid imaging condition to produce high-resolution images of the source along both space and time axes. This method gives information on the source origin time but does not provide information on the source-time function itself.

In this work, we propose a new method to simultaneously estimate both the source location and the source-time function. In particular, we aim to develop a method that requires only a smooth background velocity model and is robust in the presence of noise. Our approach is based on the co-sparsity property (Nam et al., 2013) of the physics of waves. Co-sparsity of a signal  $\mathbf{u}$  corresponds to the property that there exist a so-called analysis operator  $\mathbf{\Omega}$  that maps  $\mathbf{u}$  to a vector  $\mathbf{z}$  with few non-zero coefficients. In the context of waves, the finite-difference modelling operator acts as an analysis operator for wavefields. This implies that wavefields under the action of a finite-difference modelling kernel can be focused to sources generating these wavefields (Figure 1). We exploit this property of wavefields to locate microseismic events and estimate the source time function jointly. To arrive at a computational feasible scheme, we use the Linearized Bregman (LBR) algorithm (Yin et al., 2008; Lorenz et al., 2014; Herrmann et al., 2015) to solve the above mentioned problem.

## METHODOLOGY

FWI based methods aim to solve

$$\underset{\mathbf{f} \in \mathbb{R}^{n_x}, \mathbf{w} \in \mathbb{R}^{n_t}}{\text{minimize}} \quad \|\mathcal{F}(\mathbf{m})\mathbf{f}\mathbf{w}^T - \mathbf{d}\|, \quad (1)$$

where  $\mathcal{F}(\mathbf{m}) = \mathcal{P}\mathcal{A}(\mathbf{m})^{-1}$  is the forward modeling operator and  $\{\mathbf{f}, \mathbf{w}\}$  represent the pair of unknowns, namely the spatial component of the source  $\mathbf{f} \in \mathbb{R}^{n_x}$ , with  $n_x$  the size of the spatial grid, and source-time signature  $\mathbf{w} \in \mathbb{R}^{n_t}$  with  $n_t$  the number of time samples. The linear operator  $\mathcal{P}$  restricts wavefields to the receiver locations, followed by a vectorization.  $\mathcal{A}(\mathbf{m})$  implements a time-stepping finite-difference modelling operator, parameterized by the background squared slowness  $\mathbf{m}$ . The vector  $\mathbf{d}$  contains the set of microseismic measurements recorded at receivers either located at the surface or along a well or both. In this formulation, the spatial and time components of the source appear separable via the outer product  $\mathbf{f}\mathbf{w}^T$  with  $T$  denoting the transpose. This special structure allows Kaderli et al. (2015) to treat the spatial and temporal components of the source separately and estimate them in an alternating fashion. The obvious limitation of this approach is that it can not

## Sparsity-promoting source estimation

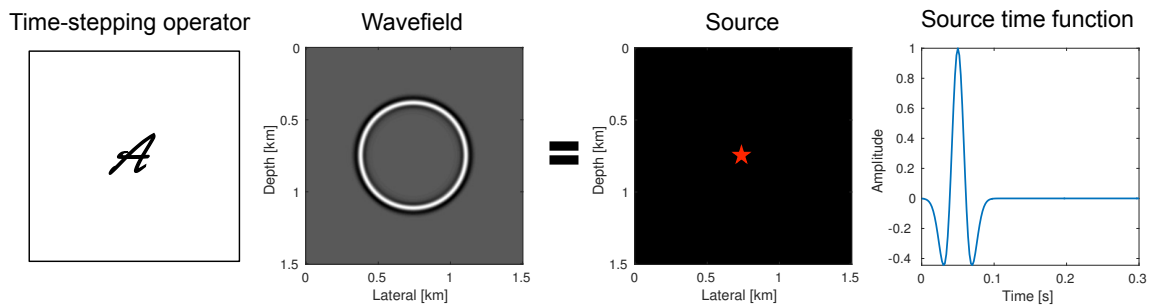


Figure 1: Schematic diagram showing time-stepping finite-difference modelling operator acting as a sparsity promoting operator on the wavefield. A snapshot of time domain wavefield is shown. The source location is indicated by the outlier (red star) corresponding to the maxima in the intensity plot and the source time function corresponds to the temporal variation of the estimated wavefield at the maxima of the intensity plot.

estimate both unknown vectors simultaneously and another limitation is that it can only work when multiple sources have the same signature. This method can be extended for multiple source cases by using a separable higher rank approximation, where the rank will be equal to the number of sources. Another obvious limitation of this extended method is that we need prior information about the number of sources.

Instead of using the separable rank-one or higher rank approximation, we use a lifting technique that is linear for a single matrix  $\mathbf{Q}$ , which contains the spatial-temporal distribution for different sources—i.e. the  $(i, j)$  entry in  $\mathbf{Q}_{i,j} = q(x_i, t_j)$ . Although it can become expensive to handle such a big matrix instead of handling the two vectors ( $\mathbf{f}$  and  $\mathbf{w}$ ), it gives us more flexibility to simultaneously estimate both the source location and the source-time signature for multiple sources with different source signatures without having any prior assumption on the number of sources.

Kitić et al. (2016) used the fact that the wave equation is in itself an excellent sparsity-promoting transform to locate the coordinate of sound sources based on microphone recordings. We used similar approach in realistic seismic settings to jointly estimate the microseismic source-location and time-signature. For a given spatio-temporal wavefield  $\mathbf{U}$  (generated by applying the inverse of the  $\mathcal{A}(\mathbf{m})$  on a sparse source  $\mathbf{Q}$ ), the action of wave equation on this wavefield, i.e.,  $\mathcal{A}(\mathbf{m})\mathbf{U} = \mathbf{Q}$ , acts as a sparsity-promoting transform. For a sufficiently accurate velocity model, the wave equation maps the full wavefield,  $\mathbf{U}$ , to a spatially focused source  $\mathbf{Q}$  (Figure 1). Hence, for point sources the finite-difference operator  $\mathcal{A}(\mathbf{m})$  acts as a sparsity-promoting transform in space when  $\mathbf{Q}$  contains a few point sources. By assuming sources to be localized in space and smooth along time, we solve

$$\underset{\mathbf{U}}{\text{minimize}} \quad \|\mathcal{A}(\mathbf{m})\mathbf{U}\|_{1,2} \quad \text{subject to} \quad \|\mathcal{P}\mathbf{U} - \mathbf{d}\|_2 \leq \varepsilon \quad (2)$$

with  $\varepsilon$  is the two-norm of the noise. By solving this minimization problem, we find a wavefield  $\mathbf{U}$  that has the smallest  $\ell_1$ -norm in space and smallest  $\ell_2$ -norm in time (denoted by the norm  $\|\cdot\|_{1,2}$ ) when acted upon by the wave equations while fitting the data to within  $\varepsilon$ . From the inverted wavefield, both the location of the sources and source-time signatures can readily be extracted.

To make the above optimization problem (equation 3) more tractable, we invoke a change of variables  $\mathbf{Q} = \mathcal{A}(\mathbf{m})\mathbf{U}$  so we arrive at

$$\underset{\mathbf{Q}}{\text{minimize}} \quad \|\mathbf{Q}\|_{1,2} \quad \text{subject to} \quad \|\mathcal{F}(\mathbf{m})\mathbf{Q} - \mathbf{d}\|_2 \leq \varepsilon. \quad (3)$$

For a given  $\mathbf{m}$ , Equation 3 takes the form of the classic Basis Pursuit Denoising (BPDN) Problem.

Motivated by recent successful application of the linearized Bregman (Yin et al., 2008; Lorenz et al., 2014) to least-squares migration (Herrmann et al., 2015), we relax the  $\|\cdot\|_{1,2}$  norm to a mixed  $\|\cdot\|_{1,2}$  and Frobenius norm—i.e., we solve

$$\underset{\mathbf{Q}}{\text{minimize}} \quad \lambda \|\mathbf{Q}\|_{1,2} + \frac{1}{2} \|\mathbf{Q}\|_F^2 \quad \text{s.t.} \quad \|\mathcal{F}(\mathbf{m})\mathbf{Q} - \mathbf{d}\|_2 \leq \varepsilon. \quad (4)$$

As in regular linearized Bregman, the parameter  $\lambda$  controls the trade of between the “sparsity” and regular two-norm terms. When  $\lambda \uparrow \infty$  the solution of Equation 4 approaches the solution of Equation 3. Compared to BP, Equation 4 permits a relatively simple iterative algorithm (See Algorithm 1 below), which is robust to noise.

### Algorithm 1 Linearized Bregman algorithm.

1. **for**  $k=1,2,\dots$
2.  $\mathbf{V}_k = \mathcal{F}(\mathbf{m})^T \Pi_\varepsilon(\mathcal{F}(\mathbf{m})\mathbf{Q}_k - \mathbf{d})$  //adjoint solve
3.  $\mathbf{Z}_{k+1} = \mathbf{Z}_k - t_k \mathbf{V}_k$  //auxiliary variable update
4.  $\mathbf{Q}_{k+1} = \text{Prox}_\lambda \|\cdot\|_{1,2}(\mathbf{Z}_{k+1})$  //sparsity promotion
5. **end**

In Algorithm 1, the dynamic step length  $t_k$  according to Lorenz et al. (2014) is given by

$$t_k = \frac{\|\mathcal{F}(\mathbf{m})\mathbf{Q}_k - \mathbf{d}\|_2^2}{\|\mathcal{F}(\mathbf{m})^T(\mathcal{F}(\mathbf{m})\mathbf{Q}_k - \mathbf{d})\|_2^2}.$$

The operator  $\text{Prox}_\lambda \|\cdot\|_{1,2}(c) := \arg \min_c \lambda \|b\|_{1,2} + \frac{1}{2} \|c - b\|_F^2$  is the proximal mapping (Combettes and Pesquet, 2011) of the  $\ell_{12}$  norm with  $\Pi_\varepsilon(\mathbf{x}) = \max\{0, 1 - \frac{\varepsilon}{\|\mathbf{x}\|}\} \cdot (\mathbf{x})$  the projection on to  $\ell_2$ -norm ball.

Compared to other sparsity-promoting approaches, this algorithm is relatively simple to implement and has very few tuning parameters.

## Sparsity-promoting source estimation

Line 2 in Algorithm 1 corresponds to a projection of the residual, given by forward modeling with the current estimate for  $\mathbf{Q}$  on the  $\ell_2$ -norm ball of size  $\epsilon$ , followed by injection of this scaled residual into the grid and time-stepping backwards in time with the adjoint of the wave equation. The result  $\mathbf{V}$  of this is used to update  $\mathbf{Z}$ , the auxiliary variable in line 3. To focus the resulting estimate for the source wavefield, we apply the proximal operator that sparsifies  $\mathbf{Q}$  along the spatial coordinates and that keeps the energy along time in check.

After solving for  $\mathbf{Q}$ , we obtain a final image of the locations of the microseismic events by performing a summation of absolute amplitude of the estimated  $\mathbf{Q}$  along time at each grid point. This results in an intensity plot where the source locations appear as outliers. We obtain estimates for the time-signature by extracting the temporal variations of the estimated wavefield at the spatial locations of the maxima in the intensity (Figure 1).

### NUMERICAL EXPERIMENTS

We performed two different experiments in order to demonstrate the ability of proposed algorithm. For both the experiments we used 3 layered synthetic velocity model of dimension  $0.9\text{km} \times 0.7\text{km}$  ( $181 \times 141$  points) (Figure 2a & 4a). We used time-stepping finite-difference modelling method to generate microseismic data. For both the experiments we used receivers at 20.0m depth from the top surface and separated by 10.0m (Figure 2a & 4a) to record the data. For all these experiments we assume that both the source location and source time function are unknown.

#### Experiment 1—True velocity experiment

In the first experiment, we estimate the source location and source-time function using noise-free synthetic microseismic measurements. Here, we assume that we know the true velocity. We use a single source located at (0.25 km, 0.27 km) (Figure 2a) with Ricker wavelet of peak frequency 20.0Hz to generate data (Figure 3) of record length 1.0s. We compare our method with the FWI based (Kaderli et al., 2015) method. We assume that both the source location and the source-time function are unknown. We performed 20 iterations each of Linearized Bregman (LBR) and FWI with 4 inner iterations for each of unknown source location and unknown source wavelet in case of FWI. Starting with zero initial guess our method gives a focused source location (Figure 2b) in comparison to the FWI-based method (Figure 2c). Moreover, our method is able to give a good estimation of the source-time function (Figure 2d) in comparison to FWI, which looks noisier and shifted in comparison to the true wavelet. For the FWI-based method, we started with an initial guess of source wavelet as Ricker wavelet of 20.0Hz (centred at 0.2s).

#### Experiment 2—Smooth background velocity and noisy data experiment

In practice, we generally do not have a detailed velocity model. At most we have a smooth background-velocity model available. Assuming that we only have access to a smooth background-velocity model (Figure 4b), we perform this experiment. We also assume that our data is noisy. We use two sources located at (0.25 km, 0.27 km) and (0.60 km, 0.28 km) (Figure 4a) and source wavelet as Ricker wavelet with peak frequency of

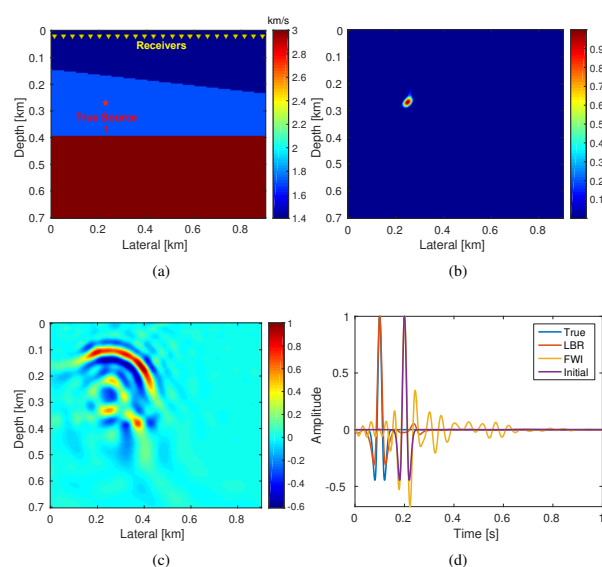


Figure 2: (a) Acquisition geometry with velocity model. Receivers are separated by 10.0m. Source location estimated by (b) Linearized Bregman as the outlier in the intensity plot, (c) FWI, (d) Comparison of normalized wavelet estimated by Linearized Bregman (LBR) and FWI with the normalized true wavelet and normalized initial guess of wavelet for FWI based method.

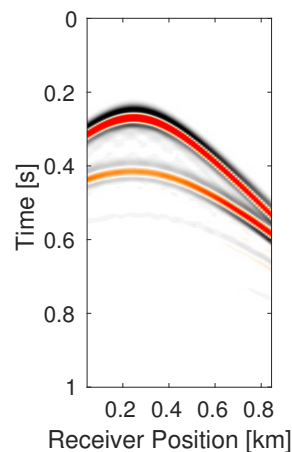


Figure 3: Noise free microseismic data generated by single source at 20.0Hz Ricker wavelet in synthetic model w/ 3 layers.

20.0Hz (centered at 0.1 s) and 15.0Hz (centered at 0.2s), respectively to generate data (Figure 5a) of record length 1.0s. We add to it low frequency (up to 45.0Hz) random noise to get the noisy data (Figure 5b) (SNR = 0.34). We use noisy data and smooth velocity to jointly estimate the source location and source time function for both sources. We perform 150 iterations each of Linearized Bregman and FWI with 4 inner iterations each for inverting for the source location and source-time function. For FWI, we use a separable rank 2 matrix

## Sparsity-promoting source estimation

(Equation 5). Here we aim to solve following rank 2 system:

$$\underset{\mathbf{f}_1, \mathbf{f}_2 \in \mathbb{R}^{n_x}, \mathbf{w}_1, \mathbf{w}_2 \in \mathbb{R}^{n_t}}{\text{minimize}} \quad \|\mathcal{F}(\mathbf{m})(\mathbf{f}_1 \mathbf{w}_1^T + \mathbf{f}_2 \mathbf{w}_2^T) - \mathbf{d}\|, \quad (5)$$

In order to decide the rank, we assume in this case that we know the number of sources a priori. Conversely, for our method, we do not need to know the number of sources a priori. With zero initial guess our method is able to give a good estimation of the location of both the sources (Figure 6a) in comparison to the FWI based method (Figure 6b). Also our method is able to give a good approximation of the true source-time function at both the locations in comparison to FWI (Figures 6c & 6d). For the FWI-based method, we started with an initial guess of the source wavelets  $\mathbf{w}_1$  and  $\mathbf{w}_2$  as Ricker wavelet with peak frequency of 20.0Hz (centered at 0.3 s) and 15.0Hz (centered at 0.4 s), respectively.

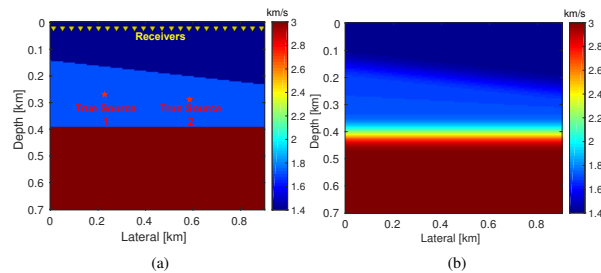


Figure 4: (a) Synthetic model w/ 3 layers along with acquisition geometry: Source 1 has a peak frequency at 20.0Hz and source 2 has a peak frequency of 15.0Hz activating delayed by 0.1 s compared to the activation of source 1 (b) Smooth background-velocity model used for source-location and source-time function estimation

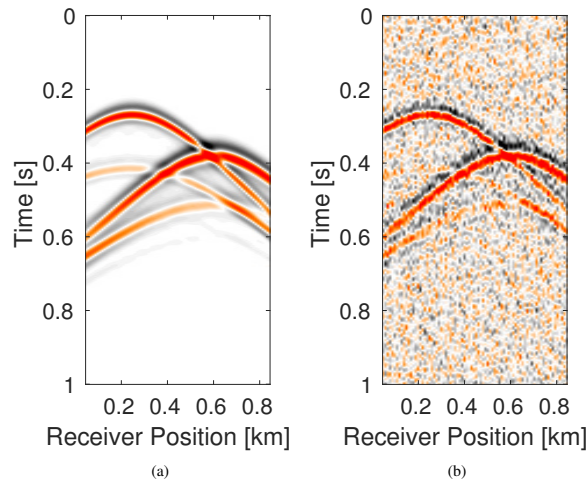


Figure 5: (a) Noise-free microseismic data generated in synthetic model w/ 3 layers by two sources with different frequencies of 20.0Hz and 15.0Hz and activating at time interval of 0.1 s and (b) Noisy microseismic data generated in synthetic model w/ 3 layers (SNR = 0.34)

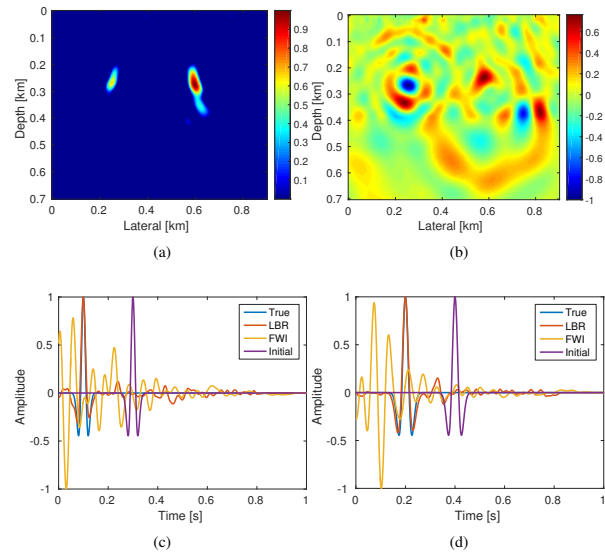


Figure 6: (a) Intensity plot showing estimated source location as two anomalies using Linearized Bregman for a smooth background-velocity model.(b) Source locations estimated by FWI using the same smooth background-velocity. Comparison of normalized wavelet estimated by Linearized Bregman (LBR) and FWI with the normalized true wavelet and normalized initial guess of wavelet for FWI based method (c) at location 1 and (d) at location 2.

## CONCLUSIONS

We have presented a new methodology to simultaneously locate microseismic events and estimate the source-time functions from surface microseismic measurements. We exploited the underlying physics of wave propagation by focusing the microseismic measurements back to its true source location. Linearized Bregman based method seems to be robust to noise and simple to be implemented with very few tuning parameters. It is also able to jointly invert for the source location and source-time function without any prior knowledge of these parameters. We demonstrated that starting with zero initial guess, even when data is noisy and we only have a smooth background velocity model available, we are able to recover accurate approximations of both the source locations and source-time functions. We also demonstrated the success of our method when we have microseismic sources with different signature.

## ACKNOWLEDGEMENT

We would like to acknowledge Mathias Louboutin for sharing the time stepping finite difference modeling code. This work was financially supported in part by the Natural Sciences and Engineering Research Council of Canada Collaborative Research and Development Grant DNOISE II (CDRP J 375142-08). This research was carried out as part of the SINBAD II project with the support of the member organizations of the SINBAD Consortium.

## EDITED REFERENCES

Note: This reference list is a copyedited version of the reference list submitted by the author. Reference lists for the 2016 SEG Technical Program Expanded Abstracts have been copyedited so that references provided with the online metadata for each paper will achieve a high degree of linking to cited sources that appear on the Web.

## REFERENCES

- Combettes, P. L., and J. Pesquet, 2011, Proximal splitting methods in signal processing, vol. 49: Springer, [http://dx.doi.org/10.1007/978-1-4419-9569-8\\_10](http://dx.doi.org/10.1007/978-1-4419-9569-8_10).
- Gajewski, D., and E. Tessmer, 2005, Reverse modelling for seismic event characterization: *Geophysical Journal International*, **163**, 276–284, <http://dx.doi.org/10.1111/j.1365-246X.2005.02732.x>.
- Herrmann, F. J., N. Tu, and E. Esser, 2015, Fast “online” migration with compressive sensing: 77th Annual International Conference and Exhibition, EAGE, Extended Abstracts, <http://dx.doi.org/10.3997/2214-4609.201412942>.
- Kaderli, J., M. D. McChesney, and S. E. Minkoff, 2015, Microseismic event estimation in noisy data via full waveform inversion: 85th Annual International Meeting, SEG, Expanded Abstracts, 1159–1164, <http://dx.doi.org/10.1190/segam2015-5867154.1>.
- Kitic, S., L. Albera, N. Bertin, and R. Gribonval, 2016, Physics driven inverse problems made tractable with cospase regularization: *IEEE Transactions on Signal Processing*, **64**, 335–348, <http://dx.doi.org/10.1109/TSP.2015.2480045>.
- Lorenz, D. A., F. Schöpfer, and S. Wenger, 2014a, The linearized bregman method via split feasibility problems: Analysis and generalizations: *SIAM Journal. Imaging Sciences*, **7**, 1237–1262, <http://dx.doi.org/10.1137/130936269>.
- Lorenz, D. A., S. Wenger, F. Schöpfer, and M. Magnor, 2014b, A sparse kaczmarz solver and a linearized bregman method for online compressed sensing: ArXiv e-prints, <http://arxiv.org/pdf/1403.7543v1.pdf>.
- McMechan, G. A., 1982, Determination of source parameters by wavefield extrapolation: *Geophysical Journal of the Royal Astronomical Society*, **71**, 613–628, <http://dx.doi.org/10.1111/j.1365-246X.1982.tb02788.x>.
- Montgomery, C. T., and M. B. Smith, 2010, Hydraulic fracturing: History of an enduring technology: *Journal of Petroleum Technology*, **62**, 26–40, <http://dx.doi.org/10.2118/1210-0026-JPT>.
- Nam, S., M. E. Davies, M. Elad, and R. Gribonval, 2013, The cospase analysis model and algorithms: *Applied and Computational Harmonic Analysis*, **34**, 30–56, <http://dx.doi.org/10.1016/j.acha.2012.03.006>.
- Rentsch, S., S. Buske, S. Lüth, and S. A. Shapiro, 2007, Fast location of seismicity: A migration-type approach with application to hydraulic-fracturing data: *Geophysics*, **72**, no. 1, S33–S40, <http://dx.doi.org/10.1190/1.2401139>.
- Rutledge, J. T., and W. S. Phillips, 2003, Hydraulic stimulation of natural fractures as revealed by induced microearthquakes, Carthage Cotton valley gas field, east Texas: *Geophysics*, **68**, 441–452, <http://dx.doi.org/10.1190/1.1567214>.
- Sjögreen, B., and N. A. Petersson, 2014, Source estimation by full wave form inversion: *Journal of Scientific Computing*, **59**, 247–276, <http://dx.doi.org/10.1007/s10915-013-9760-6>.
- Sun, J., T. Zhu, S. Fomel, and W. Song, 2015, Investigating the possibility of locating microseismic sources using distributed sensor networks: 85th Annual International Meeting, SEG, Expanded Abstracts, 2485–2490, <http://dx.doi.org/10.1190/segam2015-5888848.1>.
- Thurber, C. H., and E. R. Engdahl, eds., 2000, *Advances in seismic event location*: Springer Netherlands, <http://dx.doi.org/10.1007/978-94-015-9536-0>.
- Waldhauser, F., and W. L. Ellsworth, 2000, A double-difference earthquake location algorithm: Method and application to the Northern Hayward Fault, California: *Bulletin of the Seismological Society of America*, **90**, 1353–1368, <http://dx.doi.org/10.1785/0120000006>.

Yin, W., S. Osher, D. Goldfrab, and J. Darbon, 2008, Bregman iterative algorithms for  $\ell_1$ -minimization with applications to compressed sensing: SIAM Journal. Imaging Sciences, **1**, 143–168, <http://dx.doi.org/10.1137/070703983>.